Marine Pollution Bulletin 198 (2024) 115787

Contents lists available at ScienceDirect

Marine Pollution Bulletin

journal homepage: www.elsevier.com/locate/marpolbul

Lagrangian modelling of oil concentrations at sea: A sensitivity analysis to the grid resolution and number of Lagrangian elements

Andrés Martínez, Ana J. Abascal *, Andrés García, Germán Aragón, Raúl Medina

IHCantabria - Instituto de Hidráulica Ambiental de la Universidad de Cantabria, Santander 39011, Spain

ARTICLE INFO

Keywords:
Oil spills
Lagrangian modelling
Oil surface concentration
North Sea

ABSTRACT

This paper presents a novel method to select the optimal combination of grid resolution and number of Lagrangian elements (LEs) required in numerical modelling of oil concentrations at sea. A sensitivity analysis in terms of grid resolution and the number of LEs, was carried out to understand the uncertainty that these user-dependent parameters introduce in the numerical results. A dataset of 211,200 simulations performed under 400 metocean patterns, 6 initial volumes, 11 grid resolutions, and different numbers of LEs (100 to 500,000), was used to analyze the sensitivity of the model along different Thresholds of Concern. Results show the importance of a correct selection of the number of LEs and the grid resolution in Lagrangian modelling of surface oil concentrations. The method proposed will allow selecting the optimal combination of these parameters to find an optimal balance between the accuracy and the computational cost of the simulation.

1. Introduction

Oil and gas exploration, production and transport occur all over the world, from rivers and estuaries to seas and oceans. Accidental spills as a consequence of these activities know no borders, and the pollution caused by them poses a great risk to the coastline and marine environments. Decision-makers need technical and methodological tools, including the results of numerical models, to examine the potential impacts and the necessary response equipment in areas dedicated to oil exploration, extraction or production, and transport. At a national or regional level, knowing the sources from which a spill can originate and the potential area of affection, as well as forecasting oil transport and fate in case of an accident is essential to improve oil spill prevention and response. Thus, oil spill numerical models are a key element of the risk assessment required in planning and preparedness, as well as for the spill prediction required in response operations.

Nowadays, there are a large number of mathematical models that simulate the transport and fate of oil slicks (e.g. Daniel et al., 2003; Abascal et al., 2007; Beegle-Krause, 2001; Mínguez et al., 2012; De Dominicis et al., 2013a; Fernandes et al., 2013; Dagestad et al., 2018; Chiri et al., 2020). Oil spill models' capabilities range from the prediction of surface transport (winds, currents, and oil drift) to full 3-D processes that include oil fate and environmental effects (Barker et al., 2020; Keramea et al., 2021). Most of the state-of-the-art oil spill models use Lagrangian formulation to compute oil transport (advection and dispersion) and individual formulations to compute oil weathering processes. The Lagrangian approach involves representing oil slicks by Lagrangian elements (LEs) or particles that are transported by advection and dispersion. The oil spill is also affected by weathering processes, such as spreading, evaporation, emulsification, dispersion, dissolution, biodegradation, photo-oxidation, and sedimentation that impact the oil mass balance and the oil concentrations in the marine environment.

As a result, Lagrangian models provide the transport and dispersion of oil slicks over time, represented by a cloud of points or particles on a map. However, for response needs and other analyses, it is desirable to obtain the results in a Eulerian framework, i.e. the oil concentration (mass per unit area or volume) over the region of interest, at a scale appropriate to that of the incident. Oil spill concentration maps, especially over a Threshold of Concern (ToC), provide important information for oil spill responders to assess the consequences and potential impacts of oil spills. The threshold for toxic effects is highly variable depending on the impact and consequences of the spill. For example, effects on socioeconomic resources may occur (e.g., fishing may be prohibited) if oil is visible on the water surface ($\geq$0.1 g/m^2). Effects on wildlife (birds, mammals, and reptiles) may occur if the density of oil on the water surface is $\geq$10 g/m^2 (French-McCay, 2016; French-McCay et al., 2018; French-McCay et al., 2022). Modelling oil concentrations requires the projection of the mass transported by Lagrangian elements onto a

* Corresponding author.
E-mail address: abascalaj@unican.es (A.J. Abascal).

https://doi.org/10.1016/j.marpolbul.2023.115787
Received 23 May 2023; Received in revised form 7 July 2023; Accepted 11 November 2023
Available online 23 November 2023

Eulerian grid (Barker et al., 2020). Although some methods have been developed to provide this information without dependence on grid size (Galt, 1994; Björnham et al., 2015), most of the methods to calculate gridded concentrations depend on the choice of the number of LEs (or particles) used and on the desired horizontal or vertical grid resolution (D'Amours et al., 2015; Barker et al., 2020). Thus, most oil spill numerical models nowadays calculate the concentration of oil from the number of particles within each grid cell, hereafter called the box-counting method (Korotenko et al., 2004; De Dominicis et al., 2013a, 2013b; Gonçalves et al., 2016; Periáñez, 2020; Calzada et al., 2021; French-McCay et al., 2021; Abascal et al., 2022).

This transformation from a Lagrangian to a Eulerian approach is identified as an important uncertainty source in oil spill modelling (Barker et al., 2020; Keramea et al., 2021). The selection of the grid size and the number of LEs is user-dependent and arbitrary and must be done with care to avoid biased results, especially in the numerical modelling of oil concentrations.

Besides its relevance for the accuracy of the modelling results, the number of LEs has also an important influence on the computational cost of the Lagrangian modelling. The higher the number of particles, the higher the computational costs required for oil spill modelling. This cost can be particularly high, and even a limiting factor, in medium and long-term simulations and for stochastic modelling, such as that required to assess the risk associated with deep-sea offshore oil spills (Chiri et al., 2019, 2020). Typically, uncertainty quantification in oil spill modelling is mainly focused on the impact of inputs, especially wind, waves, and current fields, as well as model coefficients in the trajectory and dispersion of the oil slick (Abascal et al., 2009a, 2009b, 2012, 2017a, 2017b; French-McCay et al., 2021; De Dominicis et al., 2013b; Gonçalves et al., 2016; Kampouris et al., 2021). There are a limited number of studies focused on the uncertainty of Lagrangian oil spill simulations associated with model configuration in terms of grid resolution and the number of LEs used to represent the oil slick, and especially, to simulate oil concentrations. De Dominicis et al. (2013b) analysed the sensitivity of oil concentration to uncertain input parameters, number of particles, and grid resolution. The authors compared the simulations with the area occupied by two slicks observed by satellite images on August 6th and 7th, 2008. Since the analysis was focused on a specific date, metocean and spill conditions, the results may not be applied to other metocean and spill scenarios. French-McCay et al. (2021) used satellite imagery to estimate the amount and distribution of floating oil over time for comparison with model's predictions carried out during the Deepwater Horizon Oil Spill. Although numerical concentration distributions were compared to observations, their work focused on the influence of physical forcing data (currents and winds) on distributions of surface and shoreline oil.

To further advance in the numerical modelling of oil concentrations, the main goal of this study was to analyze the optimal configuration of Lagrangian oil spill modelling in terms of grid resolution and the number of particles with a twofold objective: i) to provide accurate simulations of surface oil concentrations and ii) to optimize the computational cost. A dataset of 211,200 oil spill simulations carried out in the North Sea, under different metocean conditions (400 scenarios), oil spill volumes (50 m^3 to 5000 m^3), grid resolutions (0.005° to 0.1°), and number of particles (100 to 500,000) were used to analyze the sensitivity of oil concentration over different ToC (no threshold, 0.1 g/m^2, 1 g/m^2) to the number of particles and grid resolution. Based on this analysis, this study provides a novel and simple method to obtain the optimal number of particles required for a specific grid size to simulate an oil spill volume, and achieve accurate oil concentration results while preserving computational efforts.

2. Data and methods

2.1. General overview

To achieve the aforementioned objectives, the methodology applied for the analysis was based on: i) long-term hindcast metocean databases, to consider a high number of metocean conditions; ii) oil spill numerical modelling of a high number of scenarios defined as the combination of grid resolution, number of Lagrangian elements (or particles), and oil spill volume and iii) an analysis of the results for different *ToC*. Fig. 1 shows a flow chart with the stages of the analysis.

The analysis was carried out in the North Sea (Fig. 2), which is a very active sea in terms of exploration, production, and transportation of oil and gas. The North Sea is a shelf sea bounded by the British Isles, Norway, and the European Continent. It has a mean depth of 74 m, two-thirds having depths shallower than 100 m (ICES, 1983). Since approximately 1960, >7800 wells have been drilled, and 44 billion barrels of crude oil extracted, on the United Kingdom's Continental Shelf alone (UKCS) (OGA, 2018). This intense activity involves a risk in terms of oil spill accidents. In 2017, for example, 253 accidental oil releases occurred on the UK's continental shelf, with a total of 23 t of crude oil spilled to the marine environment (Chiri et al., 2020). This activity and the associated oil spill risk motivated the study site selection.

As shown in Fig. 1, the analysis involved the following steps:

1. Metocean data. The first step of the methodology was to select the metocean conditions that will represent the forcings for the oil spill simulations. For this purpose, long-term reanalysis databases (27 years) of wind and surface currents are used to obtain a representative set of metocean (wind and currents) patterns in the study site. Note that given the spatial scale of application of the model, the Stoke's drift was discarded with respect to the effect of winds and currents on the oil spill transport (Abascal et al., 2017b; Chiri et al., 2020). Following Chiri et al. (2020), the *k*-means technique was applied to extract the *k* most relevant spatio-temporal patterns of coincident wind and surface currents during a 30-day period from the reanalysis dataset, each one of them with a specific probability of occurrence. These *k* metocean patterns (wind and surface currents) represented the forcings for the oil spill simulations.
2. Modelling methodology. Once the metocean patterns were selected, a set of spill modelling scenarios based on the combination of spatial resolution values of the grid (*i*), number of Lagragian elements or particles (*m*), and oil spill volumes (*n*) were established. Each spill modelling scenario was run for the *k* metocean patterns for a 30 day period using a Lagrangian oil spill numerical model. Based on Chiri et al. (2020), a hypothetical spill point located at 3.55°N, 56.187°E was selected as the initial location of the spill simulations (see Fig. 2). As a result, a dataset of $N = k\ x\ i\ x\ m\ x\ n$ oil spill simulations that provided the evolution of the surface oil concentration of the spilled oil was provided. In order to have a reference framework to evaluate the differences observed in the numerical modelling of the different scenarios, a high-quality and demanding configuration was established based on a high-resolution grid (0.005°) and a high number of particles (500000). The use of high-resolution grids and a large number of particles usually provide more accurate numerical simulations than coarse grids and a low number of LEs (e.g. Nagheeby and Kolahdoozan, 2010; De Dominicis et al., 2013b). Based on this hypothesis, this configuration was considered the best approach from the numerical point of view and used as reference (benchmark) to compare the results of the different model configurations. The benchmark configuration as well as each spill scenario combination (defined by volume, grid resolution, and number of LEs) were simulated for the *k* metocean patterns.
3. Results. For each spill scenario, the relative error (E_r) between the modelled spill scenarios and the benchmark simulation (same volume, 0.005° grid resolution, 500,000 LEs) was calculated for all the

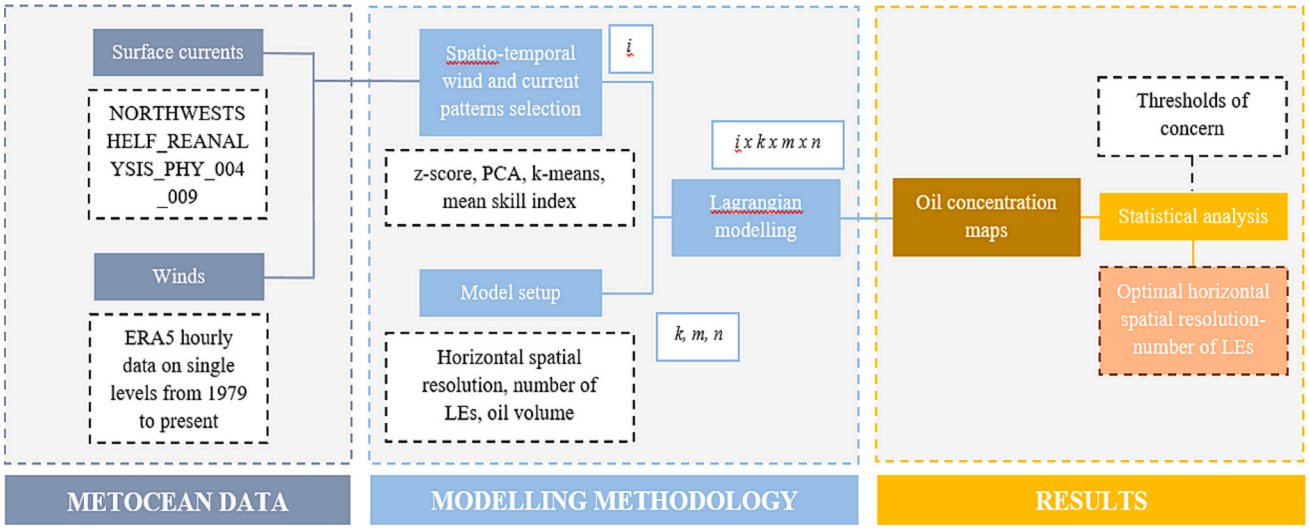

Fig. 1. Flow chart of the methodology applied for the analysis.

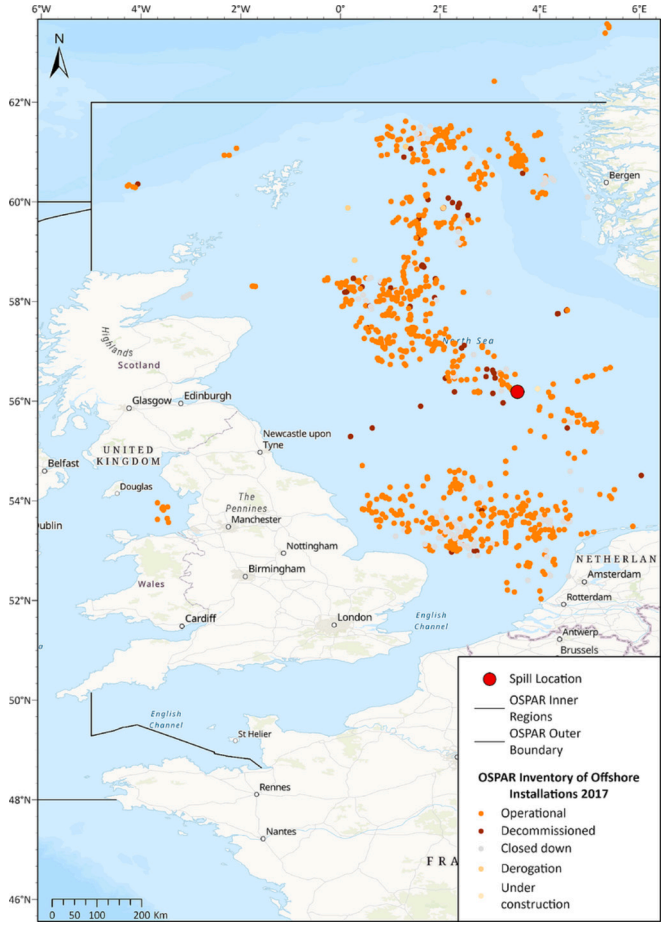

Fig. 2. Map of the study area showing the location of offshore platforms in the area (orange circles) (Source: https://odims.ospar.org/en/maps/map-inventory-of-offshore-installations-2017/). The red circle represents the spill location considered in this study. (For interpretation of the references to color in this figure legend, the reader is referred to the web version of this article.)

metocean scenarios. This comparison was carried out without ToC and considering ToCs of 0.1 g/m^2 and 1 gr/m^2, respectively (French-McCay et al., 2014). As a result, a relative error for each combination of spill volume, grid resolution, number of particles, and ToC was provided and used to identify the optimal combination of grid resolution and number of particles to simulate the surface oil concentration.

2.2. Metocean data

Surface currents were obtained from the Copernicus Marine Environment Monitoring Service (CMEMS) ocean physics reanalysis for the North-West European Shelf «NORTHWESTSHELF_REANALYSIS_PHY_004_009» product (https://marine.copernicus.eu/). The product is provided as daily, de-tied, averages. It has a vertical coverage from −5000 m to 0 m (24 z-levels). Surface currents were extracted at a nominal depth of 0 m. Data are available with a horizontal resolution of 0.111° x 0.067°, a daily mean temporal resolution, and a temporal coverage ranging from 1992 to 2018.

Wind data at a height of ten meters above ground level were obtained from the ERA 5 dataset (Hersbach et al., 2020), available at the Copernicus Climate Change Service (C3S) Climate Data Store. ERA5 is the fifth-generation European Centre for Medium-Range Weather Forecasts (ECMWF) global weather and climate reanalysis and replaces ERA-Interim reanalysis (Dee et al., 2011). It provides a wide range of atmospheric, land-surface, and sea-state parameters. Data are available with a horizontal spatial resolution of 0.25° x 0.25°, an hourly temporal resolution, and a temporal coverage spanning from 1979 to date.

All datasets were extracted for the same domain (shown in Fig. 2) and temporal coverage, spanning from 1992 to 2018 (27 years). 24-hour averages of wind data were calculated to have the same temporal resolution as the current data.

2.3. Spatio-temporal wind and current patterns selection

The met-ocean variability of a specific study area based on historical reanalysis databases is usually obtained using the Monte Carlo method (Abascal et al., 2010; Liubartseva et al., 2015) or by extracting metocean fields from the databases every specific time (Canu et al., 2015; Androulidakis et al., 2020). These methods are based on the selection of a high number of metocean scenarios and, consequently on a high number of oil spill simulations, which increases with the temporal length of the historical database. As an example, Canu et al. (2015) calculated hazard maps for the island of Sicily (Italy) by performing an ensemble of 730 oil spill simulations, each driven by a slightly different (1-day shifted) circulation field extracted from a 2-year period met-ocean database.

Given the high temporal coverage (27 years) of the historical

databases used in this work, the application of this approach would involve a large number of oil spill simulations. To optimize the number of simulations, the selection of the most relevant environmental conditions at the study site has been carried out following the methodology developed by Chiri et al., 2020. This methodology, based on the application of data mining techniques, allows considering and managing very extensive historical met-ocean databases and optimizes the computational efforts of the oil spill modelling by only considering those specific met-ocean scenarios characteristic of the study domain.

Therefore, a set of patterns of simultaneous evolution of wind and surface currents representative of the 27-year dataset were selected following the methodology developed by Chiri et al. (2020). Based on this work, the *k*-means algorithm was applied to select spatio-temporal patterns of coincident wind and surface currents during a 30-day period, which is the simulation period of the oil spill model. As a first step, a single matrix (*M*0) merging the reanalysis data was created (see Table 1). Thus, if n_w and n_c are the number of elements of the wind and surface current arrays-matrices (daily data), respectively, and T is the number of time steps of reanalysis data, the raw data matrix *M*0 will have dimensions $(T \times (2n_w + 2n_c))$. The *u* and *v* components of the wind are expressed as ${u_{w,i}}^t$, ${v_{w,i}}^t$, where $i = 1, \ldots, n_w$ and $t = 1, \ldots, T$, while those of the current are expressed as ${u_{c,j}}^t$, ${v_{c,j}}^t$, where $j = 1, \ldots, n_c$. As result, *M*0, is a 9860 × 77,544 matrix, where the number of rows equals the number of time steps (number of days in the 27-year data period considered) and the number of columns equals the number of elements of the wind and surface current array-matrices (8480 wind array elements +69,064 surface current array elements).

The Principal Component Analysis (PCA) technique was used to reduce the dimension of *M*0 while minimizing the loss of information. As shown by Chiri et al. (2020), the application of PCA facilitates subsequent steps of the analysis and improves the performance of the *k*-means algorithm. PCA projects the raw data onto a series of Principal Components (PCs). Each PC is a unit vector whose direction maximizes the variance of the projected data. The direction of the *i-th* PC is orthogonal to that of the *i*-1. The PCA is sensitive to the variance of the raw data. Therefore, each column of *M*0 must be standardized before applying the PCA. The z-score was used for its standardization so that each column in the data matrix had a mean equal to 0 and a standard deviation of 1. As a result of applying PCA to matrix *M0*, if *N* is the number of PCs obtained to explain a percentage of the original data variance, then *M0* is reduced to a new matrix *M1* of dimensions $(T \times N)$ (Table 2). Therefore, the raw data matrix was reduced to 9859 PCs. Based on previous studies (Antolínez et al., 2016; Camus et al., 2016; Chiri et al., 2019, 2020), the PCs that explained 95 % of the variance of the original data were considered. The dimensionality of the raw data matrix was reduced to 676 PCs. *M*0 was reduced to a new matrix *M*1 of dimensions 9860 × 676.

As previously mentioned, the simulation period was 30 days. Before applying the *k*-means algorithm, the sliding window method with a window duration of 30 days was applied to *M*1. To do so, if the temporal evolution of the spatio-temporal patterns that want to be obtained corresponds to *D* (30 days) time steps, then a new matrix *M2* must be created by rearranging *M1* to the dimensions $(T - D) \times (N \times D)$ (Table 3). Consequently, the data (*M*1) was reorganized into a new matrix, *M*2, 9831 × 20,280 in size, which was the input matrix for the cluster analysis. The clusters that resulted from applying the *k*-means algorithm to *M*2 represented the most relevant spatio-temporal patterns, with 30 days of temporal coverage, from the available dataset.

Table 2
Matrix *M1* obtained as a result of applying PCA to *M0*.

PC_1^1	PC_2^1	…	PC_N^1
PC_1^2	PC_2^2	…	PC_N^2
⋮	⋮	⋮	⋮
PC_1^T	PC_2^T	…	PC_N^T

The *k*-means algorithm clustering technique divides the high dimensional data space into *k* clusters or patterns, each defined by a centroid and containing the data for which the centroid is the nearest (Camus et al., 2011). To select the optimal number of patterns (*k*), a comparison was made between the synthetic data series created from the *k* clusters and the original series, for an increasing number of values of *k*. The agreement between both series was calculated based on the *d*-index (*d*) proposed by Willmott (1981), which is defined as:

$$d = 1 - \frac{\sum_{i=1}^{k} |P_i - O_i|^2}{\sum_{i=1}^{k} \left(|P_i - \overline{O_i}| + |O_i - \overline{O_i}| \right)^2} \quad (1)$$

where *O* is the original time series, and *P* is the synthetic data series. *d* varies between 0 and 1 where a computed value of 1 indicates a perfect agreement between the observed and predicted observations, and 0 connotes one of a variety of complete disagreements.

In order to optimize the number of oil spill numerical simulations to be computed, which is highly dependent on the number of metocean patterns, an optimal balance between the number of patterns and the *d*-index value has to be considered. Fig. 3 shows the evolution of the *d*-index for a number of patterns ranging from 0 to 5000. As observed in this figure, the index of agreement has a value near 0.65 for 400 patterns, indicating the good performance of the clustering technique (Willmott et al., 1985). There is no significant improvement from this point onwards, indicating that the benefit of using a higher number of patterns may not be significant. Based on this analysis, the *k*-means algorithm was applied to *M*2 to obtain the *k* (400) metocean spatio-temporal patterns from the reanalysis dataset.

It is worth noting that the obtained patterns are expressed in terms of the standardized PCs from matrix *M*2. Thus, these patterns need to be reconstructed as per the original space and by destandardizing the results. By doing so the obtained pattern can be reconstructed in the original space of matrix *M*0. The original data series can be reconstructed in accordance with the obtained patterns by considering, in each case, the closest pattern or best matching unit (BMU). Then, a probability of occurrence P_i can be calculated for each of the *k* patterns obtained. More details regarding the methodology can be found in Chiri et al. (2020).

As an example, Fig. 4 shows one of the patterns obtained. Each panel corresponds to one day, showing surface currents (black arrows) and wind (red arrows).

2.4. Oil spill model setup

The spatio-temporal patterns of wind and surface currents obtained in the previous section were used to run a state of-the-art Lagrangian oil spill model to simulate the evolution of the oil spill under different metocean conditions and to analyze the effect of grid resolution and the number of particles in the accuracy of the model's results, in terms of oil concentration.

Table 1
Raw data matrix of concurrent winds and currents (for pattern selection).

10 m u-components of wind				10 m v-components of wind				u-components of current				v-components of current			
${u_{w,1}}^1$	${u_{w,2}}^1$	⋯	${u_{w,n_w}}^1$	${v_{w,1}}^1$	${v_{w,2}}^1$	⋯	${v_{w,n_w}}^1$	${u_{c,1}}^1$	${u_{c,2}}^1$	⋯	${u_{c,n_c}}^1$	${v_{c,1}}^1$	${v_{c,2}}^1$	⋯	${v_{c,n_c}}^1$
${u_{w,1}}^2$	${u_{w,2}}^2$	⋯	${u_{w,n_w}}^2$	${v_{w,1}}^2$	${v_{w,2}}^2$	⋯	${v_{w,n_w}}^2$	${u_{c,1}}^2$	${u_{c,2}}^2$	⋯	${u_{c,n_c}}^2$	${v_{c,1}}^2$	${v_{c,2}}^2$	⋯	${v_{c,n_c}}^2$
⋮	⋮	⋮	⋮	⋮	⋮	⋮	⋮	⋮	⋮	⋮	⋮	⋮	⋮	⋮	⋮
${u_{w,1}}^T$	${u_{w,2}}^T$	⋯	${u_{w,n_w}}^T$	${v_{w,1}}^T$	${v_{w,2}}^T$	⋯	${v_{w,n_w}}^T$	${u_{c,1}}^T$	${u_{c,2}}^T$	⋯	${u_{c,n_c}}^T$	${v_{c,1}}^T$	${v_{c,2}}^T$	⋯	${v_{c,n_c}}^T$

Table 3
Matrix *M2* obtained by reshaping *M0* to consider the temporal evolution of the PCs.

PC_1^1	PC_1^2	…	PC_1^D	PC_2^1	PC_2^2	…	PC_2^D	…	PC_N^1	PC_N^2	…	PC_N^D
PC_1^2	PC_1^3	…	PC_1^{D+1}	PC_2^2	PC_2^3	…	PC_2^{D+1}	…	PC_N^2	PC_N^3	…	PC_N^{D+1}
PC_1^3	PC_1^4	…	PC_1^{D+2}	PC_2^3	PC_2^4	…	PC_2^{D+2}	…	PC_N^3	PC_N^4	…	PC_N^{D+2}
…	…	…	…	…	…	…	…	…	…	…	…	…
PC_1^{T-D+1}	PC_1^{T-D+2}	…	PC_1^T	PC_2^{T-D+1}	PC_2^{T-D+2}	…	PC_2^T	…	PC_N^{T-D+1}	PC_N^{T-D+2}	…	PC_N^T

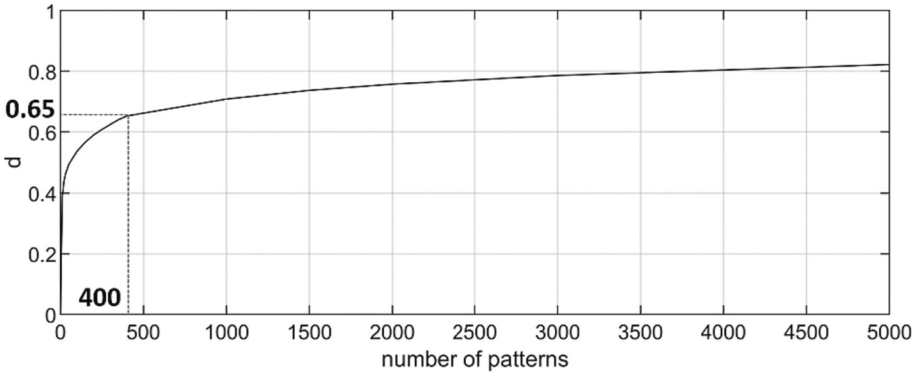

Fig. 3. Evolution of Willmott's index of agreement d with the number of patterns considered.

To do so, a set of spill scenarios defined by volume, grid resolution, and number of LEs was proposed, as shown in Table 4. The simulations were carried out considering a hypothetical spill located at coordinates 3.55°E, 56.187°N (see Fig. 2). A Brent product with a density of 832.8 kgm^{-3} and a kinematic viscosity of 3.72 cSt, was selected as representative of the type of oil that can be found in the North Sea. Therefore, the oil spill was simulated for the 400 spatio-temporal patterns of coincident wind and current data, and each of the input parameter combinations (Table 4). As result, 211,200 model runs were performed, which conformed the dataset used for the statistical analyses.

The simulations were performed with the oil spill numerical model TESEO (Abascal et al., 2007; Chiri et al., 2020). TESEO is a three-dimensional Lagrangian oil spill model to simulate the transport and weathering of oil spills as well as the drift of floating objects in marine environments. The model computes oil slick transport, diffusion, entrainment into the water column, beaching, and the weathering processes of evaporation, emulsification, and sedimentation. TESEO has been used during major real oil spill incidents, such as the Prestige (Spanish coast, 2002) and the Grande America oil spills (Bay of Biscay, 2019) and is currently implemented in operational oil risk management systems for oil and gas companies. The model has been validated with drifting buoys at regional and local scales (Abascal et al., 2007; Sotillo et al., 2008; Abascal et al., 2009a, 2009b, 2012, 2017a), and, in particular, in the North-West European Continental Shelf (Cárdenas et al., 2015; Abascal et al., 2017b).

The oil spill motion was computed by means of the transport induced by surface currents, winds, and turbulent diffusion. Given the regional scale of this study, the wave-induced Stokes drift was considered negligible. A wind drag coefficient (C_D) of 3 % and a diffusion coefficient (D) of 50 m^2s^{-1} were set according to the state-of-the-art (ASCE, 1996).

The surface oil concentration (in water) can be expressed as:

$$C_S(k,t) = \frac{\rho}{\Delta x \Delta y} \sum_{n_k} v(n_k,t) \tag{2}$$

where C_S is the surface concentration (kgm^{-2}) in the k-element of the grid, t is the time, n_k is the number of particles in the k-element of the grid, $v(n_k,t)$ are the oil particle volumes (m^3) in the k-element of the grid, and Δx, Δy are the grid resolutions in the x- and y- axes, respectively.

To ensure model stability, the time step Δt was assumed to vary with the horizontal resolution of the model grid so that an element did not travel more than one cell at each time step. Thus, Δt varied between 300 (finer grid) and 900(coarser grid) seconds (s). These parameters were kept constant and each trajectory was initialized as a single, instantaneous release of N elements (according to Table 4) and run for 30 days. Finally, the surface oil concentration in the water was stored hourly.

2.5. Sensitivity analysis of the model configuration

Based on the results of the 211,200 oil spill modelling runs, the influence of the grid's resolution and the number of particles in the modelling of oil surface concentration was analysed considering as thresholds of concern: 0 (no ToC), 0.1, and 1 g/m^2.

Note that in the calculation of surface concentrations by the box-counting method, there is a minimum number of particles required to represent values below a given ToC. Once the threshold to be used in the analysis has been decided, the minimum number of particles can be obtained as:

$$N^{min} = \frac{V_S(t_0)}{C_S{}^{max} \Delta x \Delta y} \rho \tag{3}$$

where N^{min} is the minimum number of particles required, V_s is the initial oil volume released, and C_s^{max} is the surface concentration corresponding to the ToC. If this minimum number is not met, all concentrations calculated would be above the ToC.

In order to conduct the analysis, it would be desirable to compare the results of the numerical modelling with real measurements or observations of surface oil concentration to analyze the best model configuration. However, given the lack of measurements for these comparisons, a high-quality and demanding simulation was performed based on a high-resolution grid (0.005°) and a high number of particles (500000). Previous tests for an oil spill of 5000 m^3, specific metocean scenarios, and different ToC (0.1, 1, 10, and 100 g/m^2) were carried out to analyze the convergence of the model solution (Martínez et al., 2021). This analysis shows that the differences in the numerical solutions for the lower and more restrictive ToC tend to be reduced for a high number of particles (>50,000) and high-resolution grids (>0.02°). Based on this analysis, the characteristics of the benchmark simulation were selected to guarantee the convergence of the simulation results. This simulation, considered to be optimal from the numerical point of view, was used as

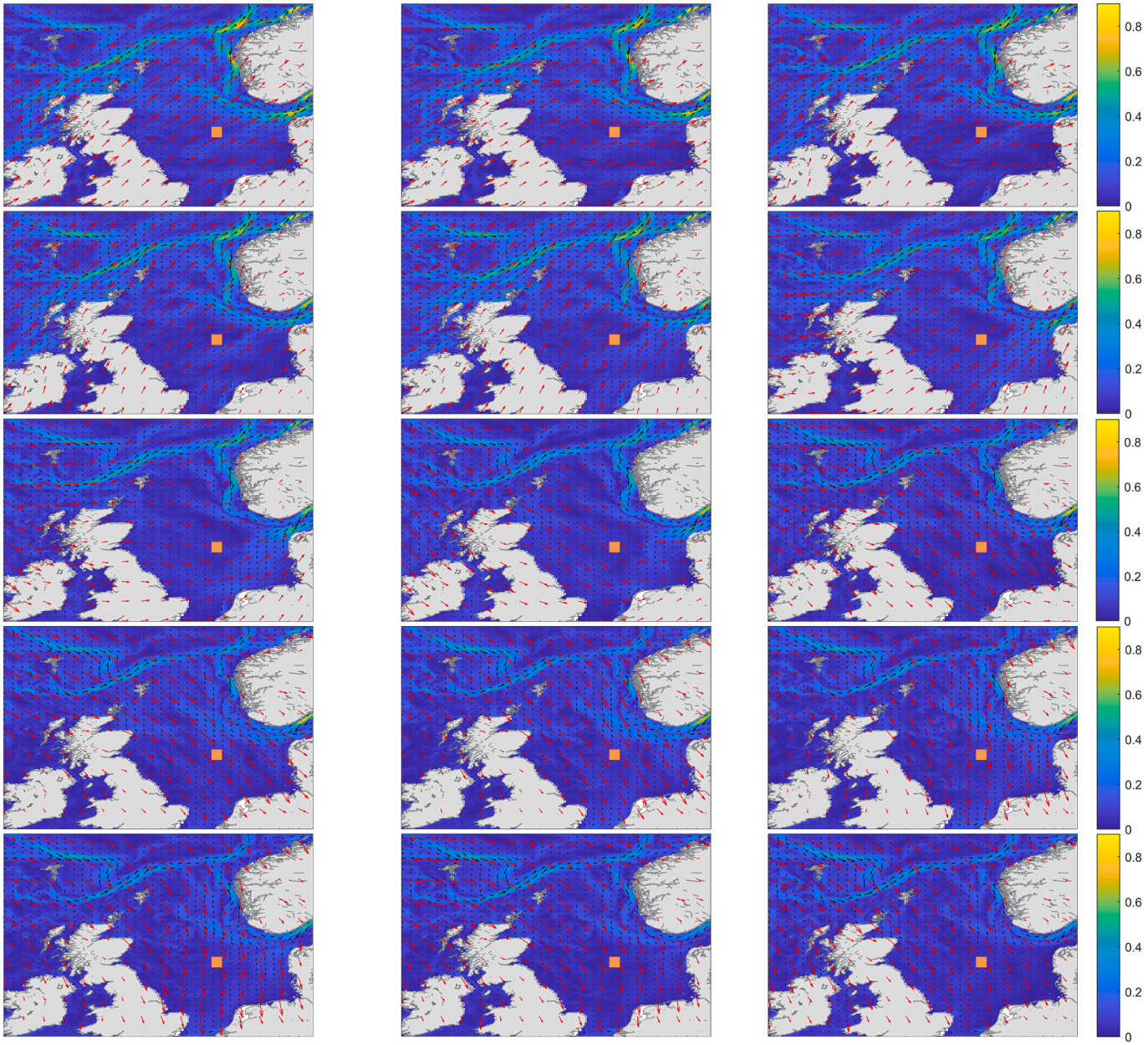

Fig. 4. Daily representation of one of the 400 spatio-temporal 30-day wind and surface current evolution patterns in the North Sea (for the purpose of clarity only the first 15 days are represented). Each snapshot corresponds to one day. Black arrows with background color maps (units in m/s) represent surface currents, red arrows refer to wind. Distances among vectors do not represent the actual resolution of the data: for clarity's sake only data of one in every five grid points, for both wind and surface currents, are represented. (For interpretation of the references to color in this figure legend, the reader is referred to the web version of this article.)

Table 4
Summary of model input parameters used for the definition of the oil spill scenarios.

Pollutant volume (m^3)	Grid resolution (°)	Number of LEs (−)
50	0.005	100
100	0.010	500
500	0.020	1000
1000	0.030	5000
2500	0.040	10,000
5000	0.050	50,000
	0.060	100,000
	0.070	500,000
	0.080	
	0.090	
	0.100	

reference (benchmark simulation) to compare the results of the different model configurations.

To illustrate it, Fig. 5 presents a comparison between the surface oil concentration maps obtained for the different configurations of the model and the benchmark simulation for an oil spill of 5000 m^3, carried out for one of the metocean patterns. The results correspond to a snapshot after 360 h of spill drift. As can be observed, a higher horizontal spatial resolution of the grid combined with a high number of particles results in a more reliable representation of the surface concentration of the pollutant in terms of continuity and smoothness of the oil slick. Therefore, the optimal result is considered to be achieved for the highest possible horizontal spatial resolution and number of LEs, in our case, a horizontal resolution of 0.005° and 500,000 LEs (upper left corner in Fig. 5).

For each spill scenario (defined by volume, grid resolution, and

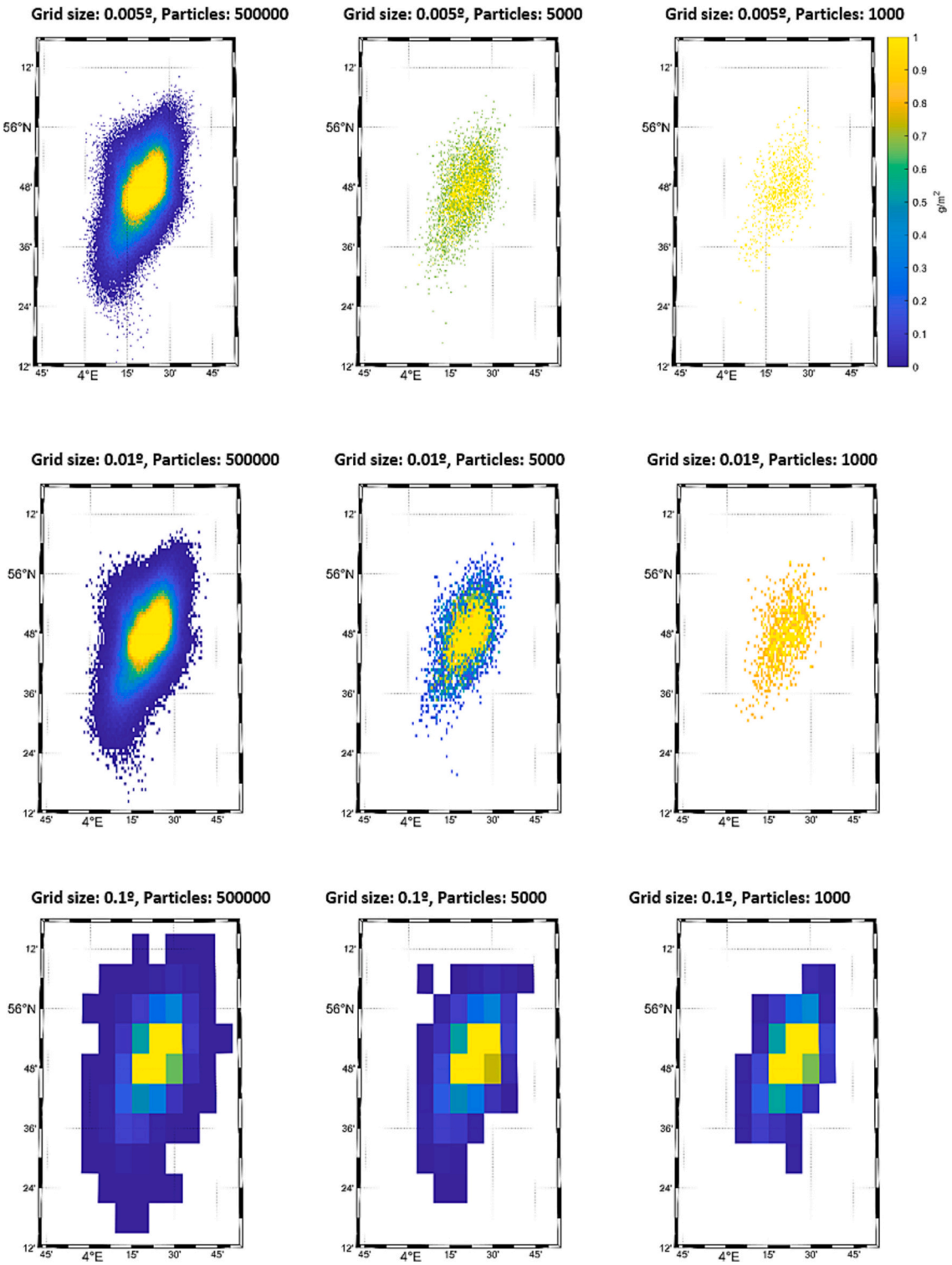

Fig. 5. Example of oil concentration obtained for different combinations of grid resolutions and number of particles. The result for the benchmark configuration is shown on the upper left corner.

number of LEs), the relative error (E_r) between the modelled scenario and the benchmark simulation (same volume, 0.005° grid resolution, 500,000 LEs) was calculated based on the following procedure:

1) Estimation of the relative error for a snapshot (E_s): for each time step, the relative surface concentration error for each grid cell (E_g) was calculated as follows:

$$E_g = \frac{|C_{esc} - C_{bm}|}{C_{bm}} \quad (4)$$

where C_{esc} is the oil surface concentration for the analysed scenario, C_{bm} is the oil surface concentration for the benchmark simulation, $g = 1, \ldots, N_g$, and N_g is the number of grid nodes of the benchmark simulation grid. Note that for the comparison of the results, C_{esc} is interpolated to the

benchmark simulation grid and only the grids with concentrations values are considered in the analysis. The result of this calculation was a grid of relative errors, with a dimension corresponding to that of the finest grid. The median of the values of the grid was calculated as a representative error of the map, i.e. $E_s = median\ (E_g)$.

2) Estimation of the relative error for a 30-days simulation (E_t): the same procedure was repeated over the entire simulated period ($T =$ 30 days), with a daily frequency. For each metocean pattern, this analysis resulted in a time series representing the temporal evolution of the relative error for the 30-day simulation period, E_{si}, where *i:1, …T*. As in the previous step, the median value was obtained as a representative value of the error in the temporal series:

$$E_t = median(E_{si}) \tag{5}$$

3) Estimation of the relative error for all metocean patterns (E_r): finally, the same procedure was repeated for each pattern of metocean conditions ($k = 400$). A series of 400 relative error data was thus obtained, each associated with the probability of occurrence of its forcing pattern (P_i):

$$E_r = \sum_{i=1}^{k} E_i P_i \tag{6}$$

Note that to carry out this analysis, the relative error associated with the 211,200 model runs (minus those excluded by the minimum number of particles) was obtained. The final result is a global relative error value (E_r) associated with each spill scenario of model input parameters (defined by volume, grid resolution, and number of LEs). These results provide a general approximation to the uncertainty expected in the modelling when these combinations of input parameters are used.

3. Results

This section presents the results of the comparison between the spill scenarios and the benchmark simulation. Section 3.1 describes the results obtained without considering a surface concentration threshold and Section 3.2 describes the result of the analysis for thresholds of 0.1 and 1 g/m^2, respectively.

3.1. Sensitivity analysis without ToC

Fig. 6 presents the relative error obtained for the different combinations of the number of particles (*x*-axis), grid resolution (*y*-axis) and volumes of 50 m^3 (left panel) and 5000 m^3 (right panel). Note that 50 m^3 and 5000 m^3 are the minimum and the maximum oil released volumes analysed. Note that when no threshold was considered in the analysis the relative error was similar for both volumes. Similar results (not shown) were obtained for the rest of the oil volumes considered, showing that the relative error was similar despite the initial volume of oil released.

Regarding the number of particles, high errors were observed when the number of particles used was low (≤ 500). In these cases, the relative error was $\geq$90 % regardless of the grid resolution adopted. Note that the simulation carried out with 1000 particles, a common practice in state-of-the-art Lagrangian trajectory modelling, leads to high relative errors ($\geq$ 75 %), suggesting that 1000 particles are not enough to accurately simulate oil spill concentrations. Fig. 6 shows that for any given grid resolution there is an optimal number of particles for which the relative error is minimum. The relative error decreases as the number of particles increases until this optimum is reached. Once this optimum has been exceeded, the error increases with the number of particles. This is explained by the combination of the small values of C_{bm} near the edges, as previously mentioned, and the additional area caused by the coarser grid. Note that the uncertainty in Lagrangian oil particle modelling is higher in the area where the particles become sparse (Björnham et al., 2015; Chen, 2022), which is more evident near the edges of the main contaminated area. Thus, the relative error may provide large values if no ToC is used to exclude the edge area where C_{bm} is very low and great uncertainty exists in the modelled particle distribution. In these cases, increasing the number of particles contributes to an increase in the relative error.

Regarding grid resolution, in general, a finer grid promotes smaller errors but requires a larger number of particles to achieve it. Thus, for a grid resolution of 0.01°, the minimum relative error is 29.21 %. However, 100,000 particles are necessary to reach this value. It is worth mentioning again that to increase the number of particles, for a 0.01° grid resolution, or to use a finer grid with the same number of particles, does not improve the accuracy in the simulation, but does increase the computational cost.

This analysis shows: i) the relevance of the selection of the appropriate combination of particles and grid resolution, both to obtain an accurate simulation as well as to optimize the computational effort, and, ii) increasing the number of particles does not necessarily improve the simulation when no ToC is considered.

3.2. Sensitivity analysis with ToC

Fig. 7 and Fig. 8 present the relative error obtained in the numerical modelling of surface oil concentration for different oil spill volumes and considering two thresholds, 0.1 and 1 g/m^2, respectively. Regarding the number of particles, on the one hand, Lagrangian modelling becomes more demanding to simulate concentrations exceeding the ToC. There is a minimum number of particles (N^{min}) required to represent the surface concentration below a given ToC (see Eq. (3)). This number depends on the ToC being analysed, the volume of product spilled, and the resolution of the selected grid. Thus, in Figs. 7 and 8, cells with no data (NaN) represent a combination of these parameters in which the number of particles is lower than the minimum required. On the other hand, and as observed without ToC, although high errors were obtained when the number of particles used was low, for any given resolution of the grid, the relative error decreased down to an optimum number of particles

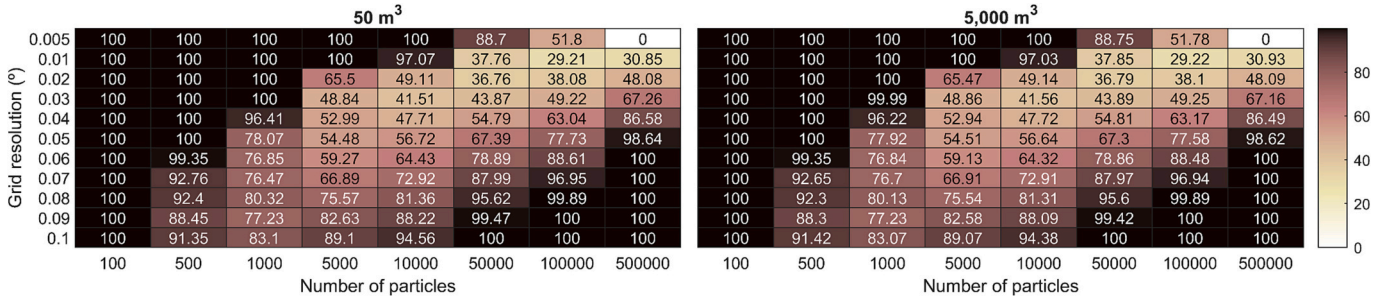

Fig. 6. Relative error in the numerical modelling of surface concentrations, depending on the horizontal resolution of the tracer grid and the number of LEs. Results for a spill volume of 50 m^3 (left panel) and 5000 m^3 (right panel) are displayed.

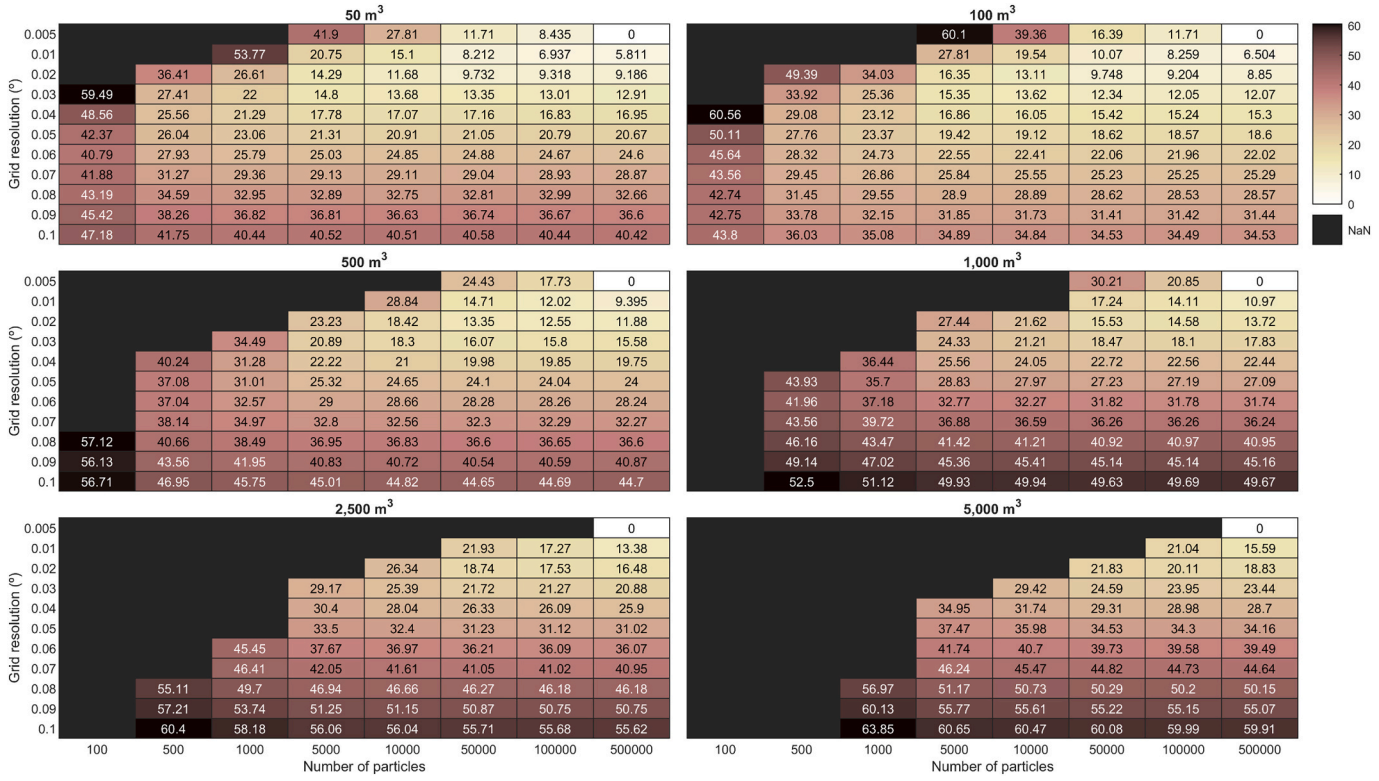

Fig. 7. Relative error in the numerical modelling of surface concentrations, depending on the horizontal resolution of the tracer grid, the number of LEs and the volume of oil spilled considering a ToC of 0.1 g/m2.

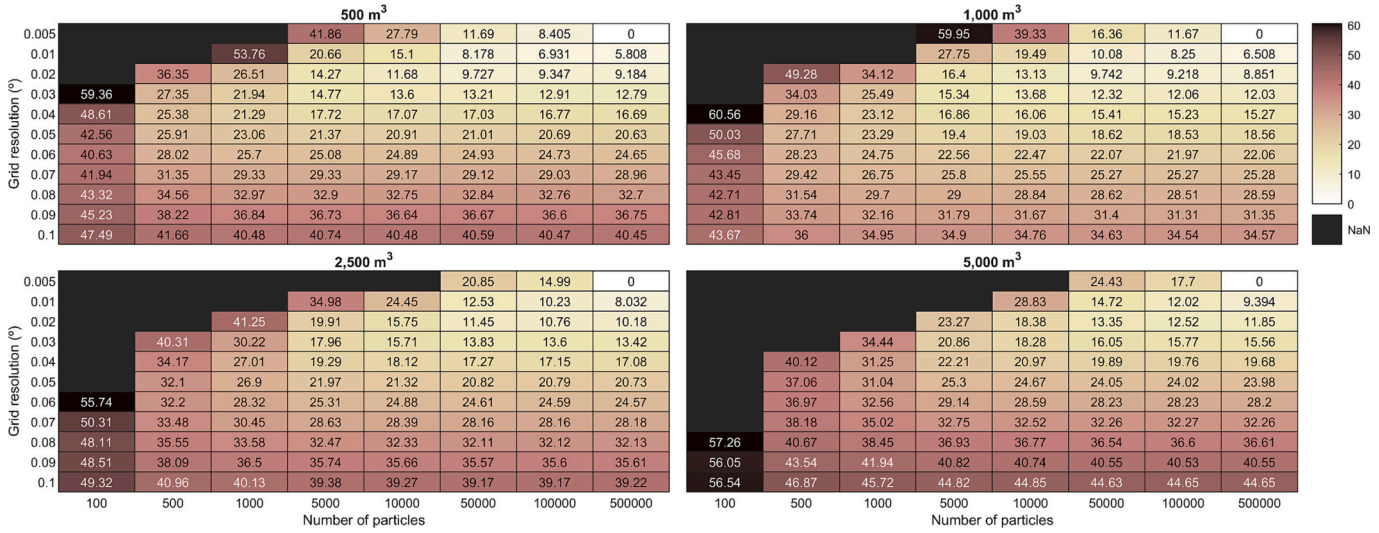

Fig. 8. Relative error in the numerical modelling of surface concentrations, depending on the horizontal resolution of the tracer grid, the number of LEs and the volume of oil spilled considering a ToC of 1 g/m^2.

from which its value stabilized or its decrease was negligible. For instance, in Fig. 7, for a volume of 1000 m^3 and a grid size of 0.05°, the relative error stabilized as of 5000 particles. Using a higher than the optimal number of particles increases the computational cost but does not improve the representation of the surface oil concentration.

Regarding grid resolution, a finer grid allows obtaining smaller errors but a larger number of particles is needed. If the number of particles is not appropriate for a specific grid resolution, it may occur that with the same number of particles a smaller error is obtained for a coarser grid. For instance, in Fig. 8, for a volume of 1000 m^3 and 50,000 particles, a larger error was obtained with a 0.005° grid (30.21 %) than with a 0.02° grid (15.53 %). This analysis shows that a high-resolution grid requires a high number of particles to obtain accurate simulations and highlights the relevance of selecting an appropriate number of particles for a specific grid size.

These findings were consistent for the two ToC analysed (0.1 and 1 g/m^2). However, the comparison of Fig. 7 (0.01 g/m^2) and Fig. 8 (1 g/m^2) shows that the relative error for the same configuration (volume, grid resolution, number of LEs) increases for lower ToCs, and when the initial oil volume released increases.

3.3. Method for the selection of model parameters

These results show that there is no specific number of particles that should be used for oil spill modelling. It depends on the initially released volume, the grid size and the ToC. Therefore, the optimal combination of grid size and number of particles should be defined according to the characteristics of the simulation. Based on the analysis carried out here, a simple and novel method is proposed for the selection of these parameters:

i) Step 1: Setting the oil spill volume;
ii) Step 2: Setting the ToC;
iii) Step 3: Setting the grid size;
iv) Step 4: Once the oil volume, ToC, and grid size are established, the number of particles that minimize the errors in the simulations is selected based on the Tables provided in Fig. 7 and Fig. 8.
v) Step 5: If computational limitations impede the use of the number of particles identified in Step 4, the user can select the appropriate combination of both parameters (based on the Tables provided in Fig. 7 and Fig. 8) to obtain the highest possible accuracy according to the computational effort that can be undertaken in the simulation.

4. Discussion

The results of this study provide new information to understand the uncertainty in Lagrangian modelling of oil concentrations at sea and a novel method to help modellers in the selection of the number of particles and grid resolution required for oil spill modelling. These parameters, required in order to represent the surface concentration in a Eulerian context, are user dependent and therefore introduce a source of uncertainty in the model's output.

Previous studies analyzing the uncertainty of Lagrangian oil spill simulations associated with the model's configuration, in terms of grid resolution and the number of LEs used to represent the oil slick, were limited and focused on specific dates, and metocean and oil spill scenarios. The analysis presented in this work is based on a comprehensive dataset of metocean conditions and numerical model's configuration, which leads to a total of 211,000 simulations that will allow establishing a reference framework for future simulations.

This section presents a discussion of the main results of the study as well as the limitations and future research required to complement the conducted analyses.

4.1. Numerical modelling of oil spill scenarios

The analysis of the 211,200 oil spill simulations shows the relevance of the selection of the appropriate number of particles for a specific grid size to optimize the accuracy of the numerical modelling as well as to optimize the computational cost of the simulation.

Leaving aside all the parameters that influence the numerical modelling of the surface oil concentration, the box-counting method performs poorly when only a few particles are used, regardless of the horizontal resolution of the grid chosen by the user, the volume of oil spilled, or the threshold of concern. Relative errors higher than 75 % were observed when no ToC was considered and the number of particles was $\leq$1000. Note that Lagrangian simulations of oil spills (Barker and Galt, 2000; Abascal et al., 2010; Keramea et al., 2022) or even of marine litter (Núñez et al., 2019; Ruiz et al., 2022a, 2022b) usually involve 1000 particles or even a lower number for longer (weeks to months) or continuous release simulations (Drouin et al., 2019; Androulidakis et al., 2020). Although previous studies (e.g. Barker and Galt, 2000; Abascal et al., 2010) have shown that 1000 particles are suitable to represent the oil slick in terms of the number of particles (or probability) that may impact a particular site, when the comparison is in terms of oil concentration the number of particles required is higher. Nagheeby and Kolahdoozan (2010) compared the concentrations provided by an oil spill model with analytical solutions using 10,000 and 100,000 particles, obtaining that accuracy increased with particle number. De Dominicis et al. (2013b) validated the results of an oil spill model with two satellite images, one for August 6th 2008 and the other observed 25 h later. They conducted a sensitivity experiment on particle number (1000, 90,000, 300,000) and grid resolution (50 m, 150 m, and 1000 m). The authors found that an oil tracer grid of about 100 m and a number of particles around 100,000 gave the best results in terms of smoothness and consistency of the simulation with the area of a satellite-detected oil slick.

Our findings agree with these studies and show that for the same initial oil volume and grid resolution, the accuracy increases with the number of LEs. However, our work also shows that this improvement is only up to a point beyond which the increase in accuracy remains constant, is negligible for concentrations above a specific threshold, or even increases when ToC is not considered in the analysis. Note that the relative error is large near the edges where C_{bm} could be very small, especially in the cases without ToC. These high E_r values near the edges, where the particles become sparse, contribute to the increase of the error with the number of particles after exceeding the optimal value. This result shows the relevance of using a ToC when modelling oil concentrations, to avoid the uncertainty caused by the scarcity of particles near the edges.

Moreover, from this point on, the use of more LEs leads to a greater computational cost, with no measurable improvement in the representation of the oil concentrations. The optimal number of LEs to achieve this maximum improvement will depend on the initial volume of oil released, the grid resolution, and the threshold of concern (see Figs. 6, 7, and 8). Our findings also show that when no ToC is considered, isolated particles can generate grid concentration values that are not realistic, even leading to an increase in simulation errors as the number of particles increases. This result suggests that to model oil concentrations, it is advisable to establish a ToC, otherwise increasing the number of particles does not necessarily improve the simulation.

Regarding the grid size, increasing the resolution generally offers a more accurate representation of the surface oil concentration. However, a finer grid does not necessarily translate into better results. When using a high-resolution grid, a large number of particles is required to avoid discontinuities in surface oil concentration values and in consequence, to provide an accurate simulation. If the number of LEs is not appropriate for a certain grid size, more accurate results can be achieved by using a coarser grid. This result is also in agreement with De Dominicis et al. (2013b), who found that the best model configuration was not associated with the maximum number of particles or the highest grid resolution, but was obtained by the right combination of both parameters.

Note that the computational cost of Lagrangian modelling increases with the number of LEs and grid resolution, and for very demanding simulations, a high number of LEs or even a finer grid size may not be computationally affordable. Thus, the results presented in Figs. 6, 7, and 8, allow the selection of the appropriate combination of grid resolution and number of particles for oil spill Lagrangian modelling by finding a balance between the accuracy required and the computational cost of the simulation.

4.2. Statistical analysis limitations

The numerical modelling of oil concentrations at sea is a highly complex process that depends on a wide variety of factors, from the properties of the oil to the formulations implemented in the numerical model. The validation of the results and more specifically, of the concentration outputs is also a complicated task, mainly due to the lack of measurements or observations available. This section analyses how these aspects influenced the analyses conducted in this study.

4.2.1. Model inputs

The oil spilled into the sea is transported by a combination of winds, currents, and waves and is affected by several physicochemical processes that depend on the oil's properties and environmental conditions. Thus, oil surface concentrations will depend on the metocean conditions, the type of product, and other model parameters, such as the wind drag coefficient C_D and the diffusion coefficient (D), not considered in this analysis.

Regarding metocean conditions, they are site-dependent. However, the use of long-term databases and the 400 30-day metocean patterns used as forcings, ensured that the modelling was carried out taking into account a wide range of metocean conditions (wind and current speed and directions), providing robustness to the analyses and allowing to establish a reference framework for other simulations.

Besides metocean conditions, oil concentrations depend to a large extent on the type of oil. An oil with a large percentage of light and volatile compounds will evaporate more readily than one with a larger amount of heavier compounds. Accordingly, light products will evaporate quicker than heavy oils, reducing the amount of oil at sea, and consequently, the oil surface concentration. Model parameters such as C_D or D also affect the transport and dispersion of the slick, and in consequence, the oil concentration. Note that to replicate the number of scenarios for the N type of oils and M combinations of other model parameters considering these issues in this study would have dramatically increased the number of simulations (N x M x 211,200), which was not feasible from the computational point of view. Therefore, further research is required to extend this analysis to other types or products (e.g. heavily or lightly refined products), and to analyze the sensitivity of the results to the model parameters. Nevertheless, the optimal combination of grid resolution and LEs provided in this study can be used as an approximation if more detailed information is not available.

4.2.2. Uncertainty estimation

As previously mentioned, the modelling scenarios have been compared with a high-quality simulation considered the benchmark simulation. This numerical comparison does not replace the validation of numerical models with oil observations and further research is required to compare the numerical results with measurements or observations, such as aerial images, remote sensing data, and field measurements. However, given the lack of observations and measurements of surface oil concentrations at sea, obtaining actual data for the 400 30-day metocean patterns analysed was not feasible. For this reason, this analysis was carried out using a numerical approach.

Note also that the relative error (E_r) associated with the various model runs represents a global value that integrates the spatial and temporal differences obtained in the simulation. For example, the grid resolution and number of particles may also depend on the sparsity of particles which usually increases with modelling time. Thus, some differences could be found in the optimal combination of grid resolution and LEs for specific periods or metocean patterns. However, the use of an aggregated index allowed us to obtain the combination of grid resolution and number of LEs to optimize the oil spill model performance as a whole.

5. Conclusions

This study presents a novel method to select the optimal combination of grid resolution and number of LEs required in numerical modelling of oil concentrations at sea, based on a dataset of 211,200 oil spill simulations.

The results of the present study show that to model oil concentrations, it is advisable to establish a ToC, otherwise increasing the number of particles does not necessarily improve the accuracy of the numerical results.

The use of few Lagrangian elements leads to noisy results, with high discontinuities in the representation of the oil concentration. In general, the use of a larger number of LEs results in a better representation of the concentration, but only up to a certain point, beyond which the improvement is reduced until it becomes negligible.

A finer grid generally offers a more accurate representation of the surface concentration. However, a large number of particles is necessary to represent surface concentration in these cases, especially below a given ToC, which translates into higher computational costs. If the number of particles is not appropriate for the grid resolution, a better representation of the surface concentration is obtained with a coarse grid than with a fine grid.

Based on these analyses, a novel and simple method for the selection of the optimal configuration of the grid and number of particles for Lagrangian modelling of oil surface concentrations is proposed in Section 3.3. For any specific oil spill simulation, this method will allow the user to: 1) be aware of the relative error incurred in the representation of the surface concentration from the number of particles and the grid resolution used in the Lagrangian modelling and, therefore, 2) select the optimal combination of these parameters so that the smallest possible error is made, depending on the computational cost that can be assumed.

CRediT authorship contribution statement

Andrés Martínez: Data analysis, Investigation, Visualization, Writing- Original draft preparation. **Ana J. Abascal:** Conceptualization, Methodology, Supervision, Writing- Original draft preparation, Reviewing & Editing. **Andrés García**: Conceptualization, Methodology, Supervision, Writing- Reviewing & Editing. **Germán Aragón**: Data analysis, Writing- Reviewing & Editing. **Raúl Medina**: Conceptualization, Writing - review & editing.

Declaration of competing interest

The authors declare that they have no known competing financial interests or personal relationships that could have appeared to influence the work reported in this paper.

Data availability

Data will be made available on request.

Acknowledgments

This work was partly carried out in the framework of the project PID2020-117267RB-I00 (COIL) funded by MCIN/AEI/10.13039/501100011033// and the project PDC2021-120892-I00 (BLOWHAZARD) funded by MCIN/AEI/10.13039/501100011033 and by European Union Next GenerationEU/PRTR.

References

Abascal, A.J., Castanedo, S., Gutierrez, A.D., Comerma, E., Medina, R., Losada, I.J., 2007. TESEO, an operational system for simulating oil spills trajectories and fate processes. In: Proceedings, ISOPE-2007: The 17th International Offshore Ocean and Polar Engineering Conference. Lisbon, Portugal, 3, pp. 1751–1758.

Abascal, A.J., Castanedo, S., Mendez, F.J., Medina, R., Losada, I.J., 2009a. Calibration of a Lagrangian transport model using drifting buoys deployed during the Prestige oil spill. J. Coast. Res. 25 (1), 80–90.

Abascal, A.J., Castanedo, S., Medina, R., Losada, I.J., Alvarez-Fanjul, E., 2009b. Application of HF radar currents to oil spill modelling. Mar. Pollut. Bull. 58, 238–248.

Abascal, A.J., Castanedo, S., Medina, R., Liste, M., 2010. Analysis of the reliability of a statistical oil spill response model. Mar. Pollut. Bull. 60, 2099–2110.

Abascal, A.J., Castanedo, S., Fernández, V., Medina, R., 2012. Backtracking drifting objects using surface currents from High-Frequency (HF) radar technology. Ocean Dyn. 62 (7), 1073–1089.

Abascal, A.J., Castanedo, S., Núñez, P., Mellor, A., Clements, A., Pérez, B., Cárdenas, M., Chiri, H., Medina, R., 2017a. A high-resolution operational forecast system for oil spill response in Belfast Lough. Mar. Pollut. Bull. 114, 302–314.

Abascal, A.J., Sanchez, J., Chiri, H., Ferrer, M.I., Cárdenas, M., Gallego, A., Castanedo, S., Medina, R., Alonso-Martirena, A., Berx, B., Turrell, W.R., Hughes, S.L., 2017b.

Operational oil spill trajectory modelling using HF Radar currents: a northwest European continental shelf case study. Mar. Pollut. Bull. 119, 336–350.
Abascal, A.J., Aragón, G., Gonzalez, M., Pérez-Díaz, B., Bárcena, J.F., Martínez, A., Pedraz, L., García-Alba, J., Largo, A.M., Lamothe, B., García, A., Medina, R., 2022. An Operational System to Forecast Marine and Atmospheric Pollution from Chemical Spills in Harbour Areas. Proceedings of the 44th AMOP Technical Seminar, Environment and Climate Change Canada, Ottawa, ON, Canada, pp. 499–513.
Androulidakis, Y., Kourafalou, V., Robert Hole, L., Le Hénaff, M., Kang, H., 2020. Pathways of oil spills from potential Cuban offshore exploration: Influence of Ocean Circulation. J. Mar. Sci. Eng. 8, 535.
Antolínez, J.A.A., Méndez, F.J., Camus, P., Vitousek, S., González, E.M., Ruggiero, P., Barnard, P., 2016. A multiscale climate emulator for long-term morphodynamics (MUSCLE-morpho). J. Geophys. Res. Oceans 121, 775–791.
ASCE, 1996. State-of-the-art review of modeling transport and fate of oil spills. J. Hydraul. Eng. 122, 594–609.
Barker, C.H., Galt, J.A., 2000. Analysis of methods used in spill response planning: trajectory analysis planner TAP II. Spill Sci. Technol. Bull. 6 (2), 145–152.
Barker, C.H., Kourafalou, V.H., Beegle-Krause, C., Boufadel, M., Bourassa, M.A., Buschang, S.G., Androulidakis, Y., Chassignet, E.P., Dagestad, K.-F., Danmeier, D.G., Dissanayake, A.L., Galt, J.A., Jacobs, G., Marcotte, G., Özgökmen, T., Pinardi, N., Schiller, R.V., Socolofsky, S.A., Thrift-Viveros, D., Zelenke, B., Zhang, A., Zheng, Y., 2020. Progress in operational modeling in support of oil spill response. J. Mar. Sci. Eng. 8, 668.
Beegle-Krause, C.J., 2001. General NOAA Oil Modeling Environment (GNOME): A New Spill Trajectory Model. IOSC 2001 Proceedings, 2. Mira Digital Publishing, Tampa, FL, St. Louis, MO, pp. 865–871.
Björnham, O., Brännström, N., Grahn, H., Lindgren, P.R., von Schoenberg, P., 2015. Post-processing of Results from a Particle Dispersion Model by Employing Kernel Density Estimation. Technical Report No. FOI-R–4135—SE. The Swedish Defence Research Agency, Stockholm, Sweden, pp. 1650–1942.
Calzada, A., Delgado de la Paz, I., Ramos, C., Lobaina, A., 2021. Lagrangian model PETROMAR-3D to describe complex processes in marine oil spills. J. Mar. Sci. 11 (01), 17–40.
Camus, P., Mendez, F.J., Medina, R., Cofiño, A.S., 2011. Analysis of clustering and selection algorithms for the study of multivariate wave climate. Coast. Eng. 58, 453–462.
Camus, P., Rueda, A., Méndez, F.J., Losada, I.J., 2016. An atmospheric-to-marine synoptic classification for statistical downscaling marine climate. Ocean Dyn. 66, 1589–1601.
Canu, D.M., Solidoro, C., Bandelj, V., Quattrocchi, G., Sorgente, R., Olita, A., Fazioli, L., Cucco, A., 2015. Assessment of oil slick hazard and risk at vulnerable coastal sites. Mar. Pollut. Bull. 94, 84–95.
Cárdenas, M., Abascal, A.J., Castanedo, S., Chiri, H., Ferrer, M.I., Sanchez, J., Medina, R., Turrell, W.R., Hughes, S.L., Gallego, A., Berx, B., 2015. Spill trajectory modelling based on HF radar currents in the North Sea: validation with drifter buoys. In: Proceedings of the 38th AMOP Technical Seminar, Environment Canada, Ottawa, ON, pp. 123–142.
Chen, H., 2022. Effect of subsea dispersant application on deepwater oil spill in the South China Sea. J. Ocean. Limnol. 40, 950–968.
Chiri, H., Abascal, A.J., Castanedo, S., Medina, R., 2019. Mid to long-term oil spill forecast based on logistic regression modelling of met-ocean forcings. Mar. Pollut. Bull. 146, 962–976.
Chiri, H., Abascal, A.J., Castanedo, S., 2020. Deep oil spill hazard assessment based on spatio-temporal met-ocean patterns. Mar. Pollut. Bull. 154.
Dagestad, K.F., Röhrs, J., Breivik, Ø., Ådlandsvik, B., 2018. Opendrift v1.0: a generic framework for trajectory modelling. Geosci. Model Dev. 11, 1405–1420.
D'Amours, R., Malo, A., Flesch, T., Wilson, J., Gauthier, J.-P., Servancks, R., 2015. The Canadian meteorological centre's atmospheric transport and dispersion modelling suite. Atmos.-Ocean 53, 176–199.
Daniel, P., Marty, F., Josse, P., Skandrani, C., Benshila, R., 2003. Improvement of drift calculation in MOTHY operational oil spill prediction system. In: Proceedings of the 2003 International Oil Spill Conference. American Petroleum Institute, Washington, D.C.
De Dominicis, M., Pinardi, N., Zodiatis, G., Lardner, R., 2013a. MEDSLIK-II, a Lagrangian marine surface oil spill model for short-term forecasting – part 1: theory. Geosci. Model Dev. 6, 1851–1869.
De Dominicis, M., Pinardi, N., Zodiatis, G., Archetti, R., 2013b. MEDSLIK-II, a Lagrangian marine surface oil spill model for short-term forecasting – part 2: numerical simulations and validations. Geosci. Model Dev. 6, 1871–1888.
Dee, D.P., Uppala, S.M., Simmons, A.J., Berrisford, P., Poli, P., Kobayashi, S., Andrae, U., Balmaseda, M.A., Balsamo, G., Bauer, P., Bechtold, P., Beljaars, A.C.M., van de Berg, L., Bidlot, J., Bormann, N., Delsol, C., Dragani, R., Fuentes, M., Geer, A.J., Haimberger, L., Healy, S.B., Hersbach, H., Hólm, E.V., Isaksen, L., Kållberg, P., Köhler, M., Matricardi, M., McNally, A.P., Monge-Sanz, B.M., Morcrette, J.-J., Park, B.-K., Peubey, C., de Rosnay, P., Tavolato, C., Thépaut, J.-N., Vitart, F., 2011. The ERA-Interim reanalysis: configuration and performance of the data assimilation system. Q. J. Roy. Meteorol. Soc. 137, 553–597.
Drouin, K.L., Mariano, A.J., Ryan, E.H., Laurindo, L.C., 2019. Mar. Pollut. Bull. 140, 204–218.
Fernandes, R., Neves, R., Viegas, C., Leitão, P., 2013. Integration of an oil and inert spill model in a framework for risk management of spills at sea: a case study for the Atlantic area. In: Proceedings of the 36th AMOP Technical Seminar, Environment Canada, Ottawa, ON, pp. 326–353.
French-McCay, D., 2016. Potential effects thresholds for oil spill risk assessments. In: Proceedings of the 39th AMOP Technical Seminar on Environmental Contamination and Response, Emergencies Science Division, Environment Canada, Ottawa, ON, Canada, pp. 285–303.
French-McCay, D., Reich, D., Michel, J., Etkin, D., Symons, L., Helton, D., Wagner, J., 2014. For response planning: predicted environmental contamination resulting from oil leakage from sunken vessels. In: Proceedings of the 2014 International Oil Spill Conference: 300108.
French-McCay, D., Crowley, D., Rowe, J.J., Bock, M., Robinson, H., Wenning, R., Walker, A.H., Joeckel, J., Nedwed, T.J., Parkerton, T.F., 2018. Comparative risk assessment of spill response options for a deepwater oil well blowout: part 1. Oil spill modeling. Mar Pollut Bull. 133, 1001–1015.
French-McCay, D.P., Spaulding, M.L., Crowley, D., Mendelsohn, D., Fontenault, J., Horn, M., 2021. Validation of oil trajectory and fate modeling of the deepwater horizon oil spill. Front. Mar. Sci. 23.
French-McCay, D.P., Frediani, M., Gloekler, M.D., 2022. Modeling emulsification influence on oil properties and fate to inform effective spill response. Front. Environ. Sci. 10, 908984.
Galt, J.A., 1994. Trajectory analysis for oil spills. J. Adv. Mar. Technol. Conf. 11, 91–126.
Gonçalves, R.C., Iskandarani, M., Srinivasan, A., Thacker, W.C., Chassignet, E., Knio, O. M., 2016. A framework to quantify uncertainty in simulations of oil transport in the ocean. J. Geophys. Res. Oceans 121, 2058–2077.
Hersbach, H., Bell, B., Berrisford, P., Hirahara, S., Horányi, A., Muñoz-Sabater, J., Nicolas, J., Peubey, C., Radu, R., Schepers, D., Simmons, A., Soci, C., Abdalla, S., Abellan, X., Balsamo, G., Bechtold, P., Biavati, G., Bidlot, J., Bonavita, M., De Chiara, G., Dahlgren, P., Dee, D., Diamantakis, M., Dragani, R., Flemming, J., Forbes, R., Fuentes, M., Geer, A., Haimberger, L., Healy, S., Hogan, R.J., Hólm, E., Janisková, M., Keeley, S., Laloyaux, P., Lopez, P., Lupu, C., Radnoti, G., de Rosnay, P., Rozum, I., Vamborg, F., Villaume, S., Thépaut, J.-N., 2020. The ERA5 global reanalysis. Q. J. Roy. Meteorol. Soc. 146, 1999–2049.
ICES, 1983. Flushing Times of the North Sea. Copenaghen.
Kampouris, K., Vervatis, V., Karagiorgos, J., Sofianos, S., 2021. Oil spill model uncertainty quantification using an atmospheric ensemble. Ocean Sci. 17, 919–934.
Keramea, P., Spanoudaki, K., Zodiatis, G., Gikas, G., Sylaios, G., 2021. Oil spill modeling: a critical review on current trends, perspectives and challenges. J. Mar. Sci. Eng. 9, 181.
Keramea, P., Kokkos, N., Gikas, G.D., Sylaios, G., 2022. Operational modeling of North Aegean oil spills forced by real-time met-ocean forecasts. J. Mar. Sci. Eng. 10, 411. https://doi.org/10.3390/jmse10030411.
Korotenko, K.A., Mamedov, R.M., Kontar, A.E., y Korotenko, L.A., 2004. Particle tracking method in the approach for prediction of oil slick transport in the sea: modelling oil pollution resulting from river input. J. Mar. Syst. 48, 159–170.
Liubartseva, S., De Dominicis, M., Oddo, P., Coppini, G., Pinardi, N., Greggio, N., 2015. Oil Spill Hazard from Dispersal of Oil along Shipping Lanes in the Southern Adriatic and Northern Ionian Seas (Mar.).
Martínez, A., Abascal, A.J., García, A., Pérez-Díaz, B., Aragón, G., Medina, R., 2021. A methodology for optimizing modeling configuration in the numerical modeling of oil concentrations in underwater blowouts: a North Sea case study. In: EGU General Assembly 2021.
Mínguez, R., Abascal, A.J., Castanedo, S., Medina, R., 2012. Stochastic Lagrangian trajectory model for drifting objects in the ocean. Stoch. Env. Res. Risk A. 26, 1081–1093.
Nagheeby, M., Kolahdoozan, M., 2010. Numerical modeling of two-phase fluid flow and oil slick transport in estuarine water. Int. J. Environ. Sci. Technol. 7, 771–784.
Núñez, P., García, A., Mazarrasa, I., Juanes, J.A., Abascal, A.J., Méndez, F., Castanedo, S., Medina, R., 2019. A methodology to assess the probability of marine litter accumulation in estuaries. Mar. Pollut. Bull. 144, 309–324.
OGA, 2018. UK oil & gas authority, wells insight report 2018. Available at. https://www.ogauthority.co.uk/media/5107/oga_wells_insight_report_2018.pdf. (Accessed December 2022).
Periáñez, 2020. A Lagrangian oil spill transport model for the Red Sea. Ocean Eng. 217, 107953.
Ruiz, I., Abascal, A.J., Basurko, O.C., Rubio, A., 2022a. Modelling the distribution of fishing-related floating marine litter within the Bay of Biscay and its marine protected areas. Environ. Pollut. 292 (A), 118216.
Ruiz, I., Rubio, A., Abascal, A.J., Basurko, O.C., 2022b. Modelling floating riverine litter in the south-eastern Bay of Biscay: a regional distribution from a seasonal perspective. Ocean Sci. 18, 1703–1724.
Sotillo, M.G., Alvarez Fanjul, E., Castanedo, S., Abascal, A.J., Menendez, J., Emelianov, M., Olivella, R., García-Ladona, E., Ruiz-Villareal, M., Conde, J., Gómez, M., Conde, P., Gutierrez, A.D., Medina, R., 2008. Towards an operational system for oil-spill forecast over Spanish waters: initial developments and implementation test. Mar. Pollut. Bull. 56 (4), 686–703.
Willmott, C.J., 1981. On the validation of models. Phys. Geogr. 2, 184–194.
Willmott, C.J., Ackleson, S.G., Davis, R.E., Feddema, J.J., Klink, K.M., Legates, D.R., O'Donnell, J., Rowe, C.M., 1985. Statistics for the evaluation and comparison of models. J. Geophys. Res. 90, 8995–9005.